Vaterite bio-precipitation induced by Bacillus pumilus isolated from a solutional cave in Paiania, Athens, Greece

ARTICLE *in* INTERNATIONAL BIODETERIORATION & BIODEGRADATION · APRIL 2015

Impact Factor: 2.13 · DOI: 10.1016/j.ibiod.2014.12.005

8 AUTHORS, INCLUDING:

Markos Daskalakis
CBI Polymers
11 PUBLICATIONS **78** CITATIONS
SEE PROFILE

Fotis Rigas
National Technical University of Athens
127 PUBLICATIONS **902** CITATIONS
SEE PROFILE

Asterios Bakolas
National Technical University of Athens, Sc…
61 PUBLICATIONS **1,159** CITATIONS
SEE PROFILE

Aristomenis P. Karageorgis
Hellenic Centre for Marine Research
93 PUBLICATIONS **1,027** CITATIONS
SEE PROFILE

International Biodeterioration & Biodegradation 99 (2015) 73–84

Contents lists available at ScienceDirect

International Biodeterioration & Biodegradation

journal homepage: www.elsevier.com/locate/ibiod

Vaterite bio-precipitation induced by *Bacillus pumilus* isolated from a solutional cave in Paiania, Athens, Greece

Markos I. Daskalakis [a], Fotis Rigas [a, *], Asterios Bakolas [a], Antonis Magoulas [b], Giorgos Kotoulas [b], Ioannis Katsikis [c], Aristomenis P. Karageorgis [d], Athena Mavridou [e]

[a] School of Chemical Engineering, National Technical University of Athens, 15700 Athens, Greece
[b] Hellenic Centre for Marine Research, Institute of Marine Biology and Genetics & Aquaculture, Heraklion, 71003 Crete, Greece
[c] Institute of Geology and Mineral Exploration, Athens, Greece
[d] Hellenic Centre for Marine Research, Institute of Oceanography, 19013 Anavyssos, Greece
[e] Technological Educational Institute of Athens, Department of Medical Laboratories, Athens, Greece

ARTICLE INFO

Article history:
Received 7 October 2014
Received in revised form
11 December 2014
Accepted 11 December 2014
Available online

Keywords:
Bacillus pumilus
Bioconsolidation
Biomineralization
Vaterite
Marble
Calcium carbonate

ABSTRACT

In this work, *Bacillus pumilus* ACA-DC 4061 was selected for its increased capability for biomineralization on marble, under different nutrient media concentrations and temperature conditions. The optimum conditions for the $CaCO_3$ bacterially-induced precipitation were determined with the aid of testing based on the Design of Experiments (DoE). Biomineral (vaterite) precipitation was favored in both the temperatures (25 and 30 °C) investigated. Stone loss rate was reduced when the samples were subjected to sonication. Thin sections of the substrate confirmed that vaterite was able to adhere onto the surface. Finally, under non-sterile conditions mimicking an *in situ* application, *B. pumilus* ACA-DC 4061 formed a fine layer of calcium carbonate. Therefore, this microorganism showed that vaterite formation may consistently occur under specific conditions and could prove useful as a candidate for on-site applications for stone conservation.

Introduction

Looking back on Earth's history, we can appreciate the role played by bacteria in its evolution (Gadd, 2010). Recent scientific proof confirms the fact that bacteria had consistently participated in calcium carbonate deposition, thus improving the environmental conditions for further evolution of life (Zavarzin, 2002). Their great importance is presented by the ongoing research with reference to their remnants in the geological samples that may shed light on the planet's formation and history (Douglas, 2005). To date, substantial research is being conducted in order to interpret the processes of precipitation of the different calcium carbonate polymorphs due to their environmental and industrial importance. Besides understanding Earth's history and cave development (Barton and Northup, 2007), this knowledge also serves to promote the various sciences, including those of surgery and dentistry (Pecher et al., 2009), biomediated soil improvement (DeJong et al., 2010) and to improve the methods of CO_2 storage (Lee et al., 2010). Stone has found extensive use as a construction material, evident from the existing architectural monuments and statues. Nevertheless, the industrial revolution has accelerated the deterioration and degradation of several stone monuments through the emission of anthropogenic pollutants that interact with the physical (rain, air, sunlight) (Pope et al., 2002; Smith et al., 2008) and biological factors (Warscheid and Braams, 2000; Scheerer et al., 2009).

Previous research had focused initially on understanding the negative effects of bacterial proliferation upon different substrates and the correlation between the physical and microbial factors. Today, the beneficial features of bacterial metabolism are being investigated for stone protection, namely their ability to promote calcium carbonate precipitation under appropriate environmental and nutrient conditions (Boquet et al., 1973). Members of the *Bacillus* genus are among those more intensively investigated due to their ubiquity in nature.

One of the first microorganisms to be investigated in light of monument bio-restoration was the heterotrophic bacterium *Bacillus cereus* (Castanier et al., 2000). Based upon the patent applied (Adolphe et al., 1990), it was studied under specific nutrient

* Corresponding author.
E-mail addresses: fotios.rigas@gmail.com, rigasf@central.ntua.gr (F. Rigas).
URL: http://www.chemeng.ntua.gr

http://dx.doi.org/10.1016/j.ibiod.2014.12.005
0964-8305/

conditions that provided the appropriate elements for calcium carbonate biomineralization. The methodology was evaluated in buildings and statues in France, and recently it was applied on plaster (Anne et al., 2010). One particular *B. cereus* strain isolated from a cave, has recently been reported to produce calcite under different nutrient conditions (Han et al., 2013).

Bacillus sphaericus possesses the advantage of the urease enzyme that, when selectively induced, promotes biomineralization (Hammes et al., 2003). Experimentation on limestone (Dick et al., 2006; De Muynck et al., 2013) and concrete (De Muynck et al., 2008a, b; Kim et al., 2013) revealed the potential of implementing this microorganism. *Sporosarcina pasteurii* (formerly *Bacillus pasteurii*), is another urease positive microorganism (Stocks-Fischer et al., 1999) tested primarily on concrete as an effective mixture component and for the bio-remediation of cracks. Results showed that although it did not provide satisfactory results for the first scenario, it could prove useful in shallow – crack remediation (Ramachandran et al., 2001). The latter, was further investigated with the application of immobilized cells in polyurethane foam (Bang et al., 2001) or premixed with sand and applied on cracks (Achal et al., 2013). A different approach to circumvent the mortality of *S. pasteurii* on concrete is the development of phenotypic mutants that can survive under conditions of high pH without the loss of ureolysis (Achal et al., 2009). The same microorganism was recently tested on bricks (Sarda et al., 2009).

Additional *Bacillus* species reported for their carbonatogenic activity are *Bacillus megaterium* (Cacchio et al., 2003), *Bacillus thuringiensis*, *Bacillus pumilus* (Baskar et al., 2006), *Bacillus pseudofirmus*, *Bacillus cohnii* (Jonkers et al., 2010), *Bacillus alkalinitrilicus* (Wiktor and Jonkers, 2011) and other *Bacillus* strains yet to be identified at the genus level (ChunXiang et al., 2010). Microorganisms from this genus have constantly been detected when selected media, which activate calcium carbonate biomineralization, were applied on quarried or decayed stone (Piñar et al., 2010; Ettenauer et al., 2011; Jroundi et al., 2012).

Investigation of the carbonatogenic ability of the isolates from stone or cave surfaces continues to remain of importance in order to understand the dynamics of the microorganisms and improve the growth media applied. Furthermore, the morphology of the biominerals deposited would assist in the differentiation between the inorganic and microbially induced biomineralization. Recently, bacterial isolates such as *B. cereus*, *Bacillus licheniformis* (Daskalakis et al., 2013) and *Cupriavidus metallidurans* ACA-DC 4073 (Daskalakis et al., 2014) were tested for their biomineralization capabilities. Similarly, we isolated and identified microorganisms isolated from a cave in Paiania, in the vicinity of Athens, Greece. One of the isolates, *B. pumilus* ACA-DC 4061, exhibited considerable biomineralization capability in the growth medium selected. Further investigations were done in order to delineate its potential to be applied on stone or exploited, if identified, in the stone microflora. Different media and growth parameters were investigated in order to detect the optimum bio-precipitation conditions and the endurance of the biomineral, which was mainly vaterite. Spraying the microorganism was tested under non-sterile conditions to partially mimic an *in situ* application and establish its potential and practicality. Finally, the statistical analysis presented and the biomineralization efficiency are discussed.

Materials and methods

Isolation, purification and genetic identification of Bacillus pumilus ACA-DC 4061

Samples for the current investigation were collected from a cave in Paiania district, near the city of Athens. The cave is accessible to visitors only during dry seasons. The following sample types were obtained: (i) cave wall material collected by sweeping the wall surface with sterile cotton swabs, which were subsequently immersed in nutrient broth; (ii) water dripping from stalactites immediately stored in sterile test tubes; (iii) non-coherent soil material from the sides of the stalagmites and (iv) water samples from a small pool of concentrated water percolating from the cave walls and stalactites hanging above. All the samples were obtained from sites far away from the visitors' walking path, lacking a direct light source and without an obvious chromatic difference. All the samples were stored immediately on ice for transport. Isolation and genetic identification were done as described previously (Daskalakis et al., 2013). The isolate, identified as *B. pumilus* ACA-DC 4061, was deposited in the Greek Bacterial Collection of Agricultural University of Athens – Greece – Laboratory of Dairy Research.

Growth media for biomineralization experiments

The basic growth medium implemented (BP1x) was 0.36 g of Bacteriological Peptone (LABM, Lancashire, UK) and 2.5 mL of 10% (w/v) calcium acetate solution [$(CH_3COO)_2Ca$ (Sigma–Aldrich, Munich, Germany)] in 100 ml deionized water. The growth media with 2x (BP2x) and 3x (BP3x) in the concentration specified above were also used during the biomineralization experiments. Liquid media were sterilized by autoclaving for 17 min at 15 psi – 121 °C. Screw-cap bottles of 250 mL capacity were filled with 100 ml of the growth medium. Qualitative observation of growth was performed by measuring the absorbance at 620 nm with a Hach DR-2000 spectrophotometer (HACH LANGE, Athens, Greece). The bacterial population (in CFU mL^{-1}) was calculated employing the serial dilution method.

Stone substrate

Marble from Penteli Mountain had been used in antiquity for several monuments and statues due to its high quality. Similar marble can be quarried only in the area of Dionysus (Daskalakis et al., 2013). Tiles made from this marble, were cut to sizes of 4 cm × 1 cm × 1–1.5 cm or 4 cm × 4 cm × 2 cm and used as the solid substrate.

Optimization of biomineralization factors

The biomineralization ability of *B. pumilus* ACA-DC 4061 was optimized through a series of tests based on the Design of Experiments (DoE). A Multilevel Factorial Design was used to construct a second order response surface with three design factors, namely, incubation temperature ($\boldsymbol{X_1}$), medium concentration as regards to bacteriological peptone – calcium acetate ($\boldsymbol{X_2}$) and inoculum concentration ($\boldsymbol{X_3}$). The design consisted of 15 trials replicated 5 times. The response selected under optimization was weight increase $\boldsymbol{Y}$ (g). The data of the statistical experiment were analyzed using the software Design-Expert 6.0.6 to determine the various components of the Analysis of Variance (ANOVA). The statistics that were used to determine whether the models, thus constructed, adequately described the experimental data included the significance of the models, lack-of-fit test and adequate precision statistic.

All the samples were analyzed for bacterial concentration, pH, calcium and acetate concentration, biomineral type and its morphology, as described below.

Optimal biomineralization experiment

The equation determined from the mathematical model mentioned above provided the optimal values regarding the

temperature, growth medium concentration and inoculum concentration. The consistency of the results was established in the final experiment, where the biodeposition process was monitored for 15 days. The inoculation of the microorganism was time zero and four samples were extracted and analyzed from the experiment once every three days.

Analysis of experimental samples

The stone samples retrieved were allowed to dry at 50 °C for 24 h prior to weighing. The quantity of calcium carbonate precipitate was calculated from the weight difference recorded before and after the treatment. Calcium and acetate monitoring, X-ray diffraction (XRD) and Fourier Transform InfraRed spectroscopy (FT-IR) of the biomineral, Scanning Electron Microscopy (SEM) and thin sections of the stone samples were analyzed as described in Daskalakis et al. (2013). Additional FT-IR analysis was performed on the biomineral samples (mainly vaterite), which were individually stored in plastic containers at room temperature for up to two years in order to detect any potential biomineral transformation (Daskalakis et al., 2014).

Weight loss with ultrasonic treatment

Biomineralized and control stone samples (from the experiments conducted under sterile conditions) were immersed in an upright position in deionized water (one of their small sides 1 cm × 1–1.5 cm was touching the bottom of the glass beaker). Sonication was applied for 5 min (40 kHz, Branson 5510, Danbury, CT, USA) and the samples were immediately rinsed with deionized water and dried at 50 °C for 24 h prior to weighing. The process was repeated five times (Daskalakis et al., 2013). The results are presented as ΔWt (%) according to the equation given below:

$$\Delta Wt(\%) = [(W\ prior\ sonic - W\ after\ each\ sonic)/W\ prior\ sonic] \times 100$$

Color measurement

The chromatic aspect of the stone after the biodeposition treatment was determined using a portable DR LANGE spectrocolor (TYPE LMG183) instrument (HACH-LANGE, Athens, Greece). Reflectance measurements were recorded at five different points on the surfaces of all treated samples and the controls after they had been subjected to sonication tests, thus providing the L^*, a^*, and b^* values. The mean value was calculated from the instrument's software (DR LANGE spectral = qc version 3.51) and used to calculate the total color difference **ΔE** applying the following equation:

$$\Delta E = \left[\Delta L^{*2} + \Delta a^{*2} + \Delta b^{*2}\right]^{1/2}$$

with **Δ** being the difference between the values of the treated samples and the values of the reference samples, which were those without the inoculum, L^* (lightness: 0 being black and 100 being diffuse white), a^* (negative values indicate green, whereas positive values indicate redness) and b^* (negative values indicate blue and positive values indicate yellow).

Evaluation of the biodeposition treatment under non-sterile conditions

The approach selected was similar to the one described previously to enable result comparability (Daskalakis et al., 2014). Briefly, six marble stone samples (4 cm × 4 cm × 2 cm) were horizontally placed on an aluminum tray creating an exposed surface area of 96 cm^2. The bacteria were re-established from the frozen stocks in the BP3x growth medium in line with the optimum growth conditions identified and prepared for spraying. Every 12 h the sample area was sprayed once with 10 ml of a three- to four-day-old bacterial culture until it was fully covered, in a concentration of the 8×10^8–1×10^9 CFU mL^{-1} range. The aluminum tray was incubated at 30 °C in a non-sterile incubator for 12 days. At the end of the experiment, a cotton swab was passed across the stone surface and the agar plates were inoculated with it to investigate if the stone surface hosted other microorganisms besides *B. pumilus* ACA-DC 4061. The stones were sprayed with sterile deionized water to remove the bacterial excess and loosely deposited $CaCO_3$. They were then dried at 50 °C for 24 h, weighed and analyzed by scanning electron microscopy (Daskalakis et al., 2014).

Results

Isolation, purification and identification of Bacillus pumilus ACA-DC 4061

Initial identification of the microorganism was successful using the API biochemical tests. Our results compared with the identification Table of API 50CHB and previous studies (Lovett and Young, 1969; O'Donnell et al., 1980; Priest et al., 1988) revealed similarities besides acid production from the galactose and xylose that were negative for our isolate. Interestingly, a negative utilization of the acetate had been previously reported (Priest et al., 1988). The isolate, however, attested to the opposite, as will be presented later. The almost full length 16S rDNA was compared in the database and the phylogenetic tree was constructed (Suppl. Fig. 1), which corresponded to *B. pumilus* (accession number JQ046373). The isolate was therefore, deposited under the name *B. pumilus* ACA-DC 4061.

Growth requirements for the biomineralization experiments

B. pumilus ACA-DC 4061 was able to grow in the bacteriological peptone medium regardless of its concentration. The growth curve is presented in Suppl. Fig. 2, with the corresponding bacterial population, performed in a 500 ml conical flask. The lag phase lasted for a few hours and the first exponential phase was a result of the assimilation of the bacteriological peptone. A second minor lag phase preceded the onset of the acetate assimilation that induced the diauxic growth after 72 h, over a 24-h period. During this time period, the bacterial population almost doubled, reaching its maximum at 7.0×10^9 CFU ml^{-1}. During acetate consumption, the solution color changed from light yellow to a white emulsion. The color change of the medium qualitatively indicated that the biomineralization process was under way.

Optimization of the biomineralization factors

After running all 60 trials of the Multilevel Factorial Design, the data produced from the statistical experiment were treated with well-established statistical diagnostics to exclude the non-acceptable ones. The final 57 runs were used to construct the coded design model of the optimization parameter (response) selected.

The significant effects of having p-values less than 0.05 (indicating that they are significantly different from zero at the 95% confidence level) were used for further analysis, while the rest were excluded from the models. Thus, the following reduced second order regression model was constructed. The model was fitted to

Table 1
Model significance, lack-of-fit test and adequate precision used to test the adequacy of the constructed statistical model.

	Model significance	Lack-of-fit	Adequate precision
Desirable values	p-value < 0.05	p-value > 0.05	Signal to noise ratio > 4
Values calculated	0.0021	0.7986	8.074

Table 2
Coded and natural values of design factors and final results of the Multilevel Factorial Design.

Design factors	−1	0	1	Optimum (coded values)	Optimum (natural values)
X_1: Temperature (°C)	25	30	35	−1.0/0.0[a]	25/30[a]
X_2: Medium Concentration (gr/100 ml)	0.36	0.72	1.08	1.0	1.08
X_3: Inoculum volume (ml)	0.5	1.0	1.5	0.0	1.0

[a] 30 °C was selected as an additional evaluation point.

the data for the coded values of the factors after previously having excluded all the insignificant effects:

$$Y_1 = 0.0478 + 0.0105X_1 + 0.0119X_2 - 0.0167X_1X_2$$

where: Y_1 is the maximum weight increase, X_1 is temperature (°C), X_2 is the medium concentration (gr/100 ml) and X_3 the inoculum volume (ml) factor.

The X_3, X_1^2, X_2^2, X_3^2, X_2X_3 and X_1X_3 factors were excluded as insignificant. The model thus derived was then tested with the statistics: model significance, lack-of-fit and adequate precision (Table 1). The results indicate that the model complied with all of the desirable values of the statistics.

The optimal value of the response was calculated from the reduced model and is shown together with the corresponding natural values of the factors in Table 2.

The model was provided with an optimum at the lowest temperature evaluated (25 °C). Nevertheless, the examination of the raw data from all the experimental series performed revealed that the highest biomineralization value was achieved at 30 °C, while the maximum at 25 °C was slightly lower. Therefore, for comparison purposes, an additional evaluation at 30 °C was performed while maintaining the other two design factors the same.

Evaluation of optimum biomineralization parameters

The starting conditions in both temperatures were similar while the color of all the media after diauxic growth transformed in a white emulsion; verifying the qualitative assessment for a successful test.

At 25 °C, acetate became part of the microorganism's nutrient source sooner than the 3rd experimental day, that the first set of samples were isolated, while at 30 °C, acetate utilization initiated after the 3rd day. In both experiments similar small amounts of acetate were unused at the end of the experiments. After day 6, the acetate assimilation is faster at 25 °C, although the end point was the same. The rate of acetate assimilation revealed a notable difference. At 25 °C, the fast rate of acetate utilization occurred until day 9, after which it decreased. However, at 30 °C, the acetate utilization increased until day 6 and then remained stable throughout the experiment (Fig. 1a). The bacterial population

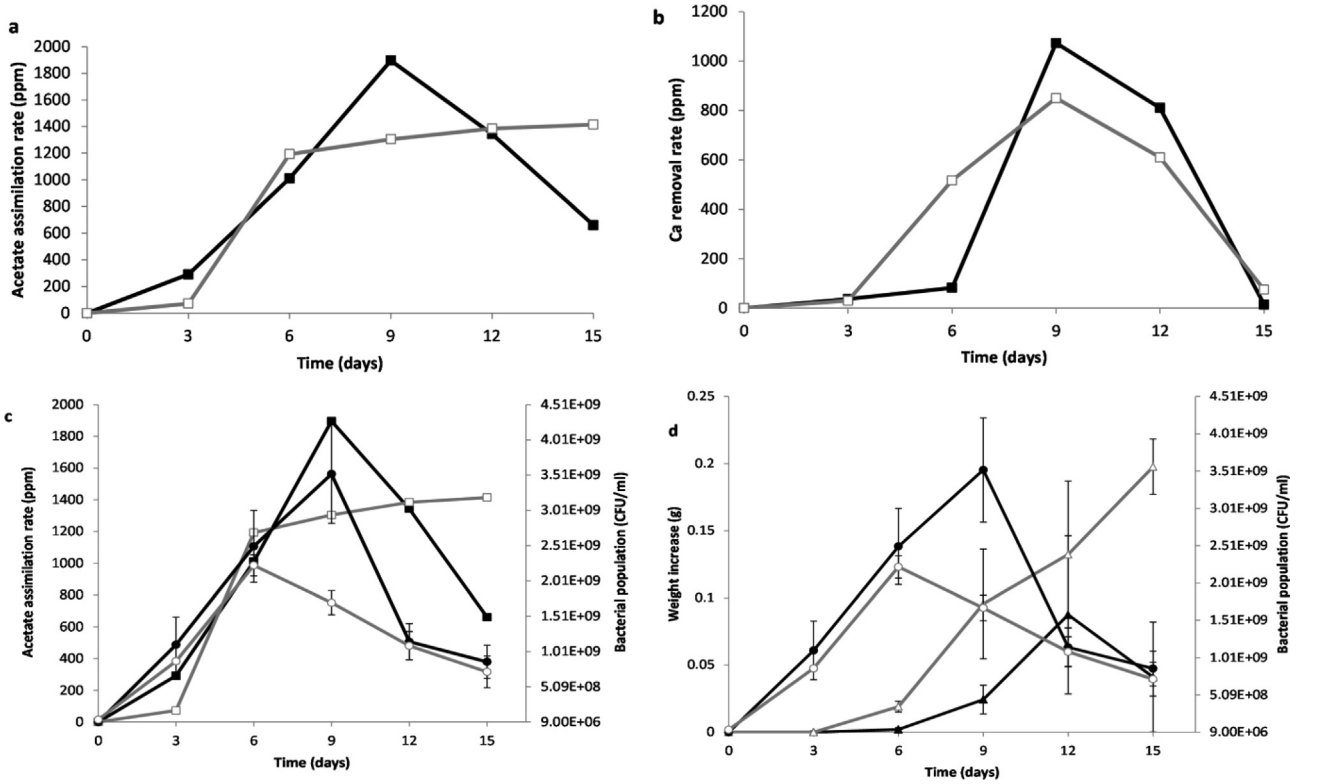

Fig. 1. Diagrams representing acetate and calcium removal, weight increase and cell density. (a) —■—: 25 °C acetate assimilation rate and —□—, 30 °C acetate assimilation rate; (b) —■—, 25 °C calcium removal rate and —□—, 30 °C calcium removal rate; (c) —■—: 25 °C acetate assimilation rate, —●—: 25 °C bacterial cell concentration, —□—: 30 °C acetate assimilation rate, —○—:30 °C bacterial cell concentration; (d) —▲—: 25 °C weight increase on marble samples, —●—: 25 °C bacterial cell concentration, —△—: 30 °C weight increase on marble samples, —○—:30 °C bacterial cell concentration. Error bars: Standard Deviation.

presented differences according to the nutrient assimilation (Fig. 1c). At both temperatures the bacteria increased in parallel with acetate assimilation. Nutrient depletion caused a sharper decrease in the cell numbers at 25 °C compared to 30 °C, while the final cell population in both experimental conditions was similar after day 12. In both temperatures, calcium removal initiated after the 3rd day, with immobilization being faster at 30 °C than at 25 °C. The calcium rate removal graph (Fig. 1b) shows that the calcium immobilization had a smoother curve at 30 °C compared with the abrupt increase between day 6 and day 9 at 25 °C. At 30 °C, the calcium was utilized for a longer time span (12 days) compared with the experiment at 25 °C (9 days). Despite the fact that at 25 °C the bacterial population increased faster and in a higher concentration, it did not result in an improved utilization of calcium for biomineralization. This exerted a direct effect upon the final degree of bio-precipitation observed (Fig. 1d). At 30 °C, the constant rate of acetate assimilation and the longer time period that calcium was part of the reaction in the solution, plus the lower numbers of the bacterial population resulted in a continuous weight increase on the marble samples throughout the entire duration of the experiment. However, at 25 °C, the biomineralization was delayed and revealed a decrease in the final sample set (day 15).

The FT-IR and XRD sample analysis under the two temperatures tested showed that at 30 °C, vaterite was the only polymorph identified throughout the experiment, whereas at 25 °C, the vaterite was observed in the samples after day 12. Prior to that, the biomineral demonstrated to be a mixture of calcite and vaterite, and in one case, a sample from day 6, calcite was the only polymorph detected. The spectra for both polymorphs are presented in Fig. 2.

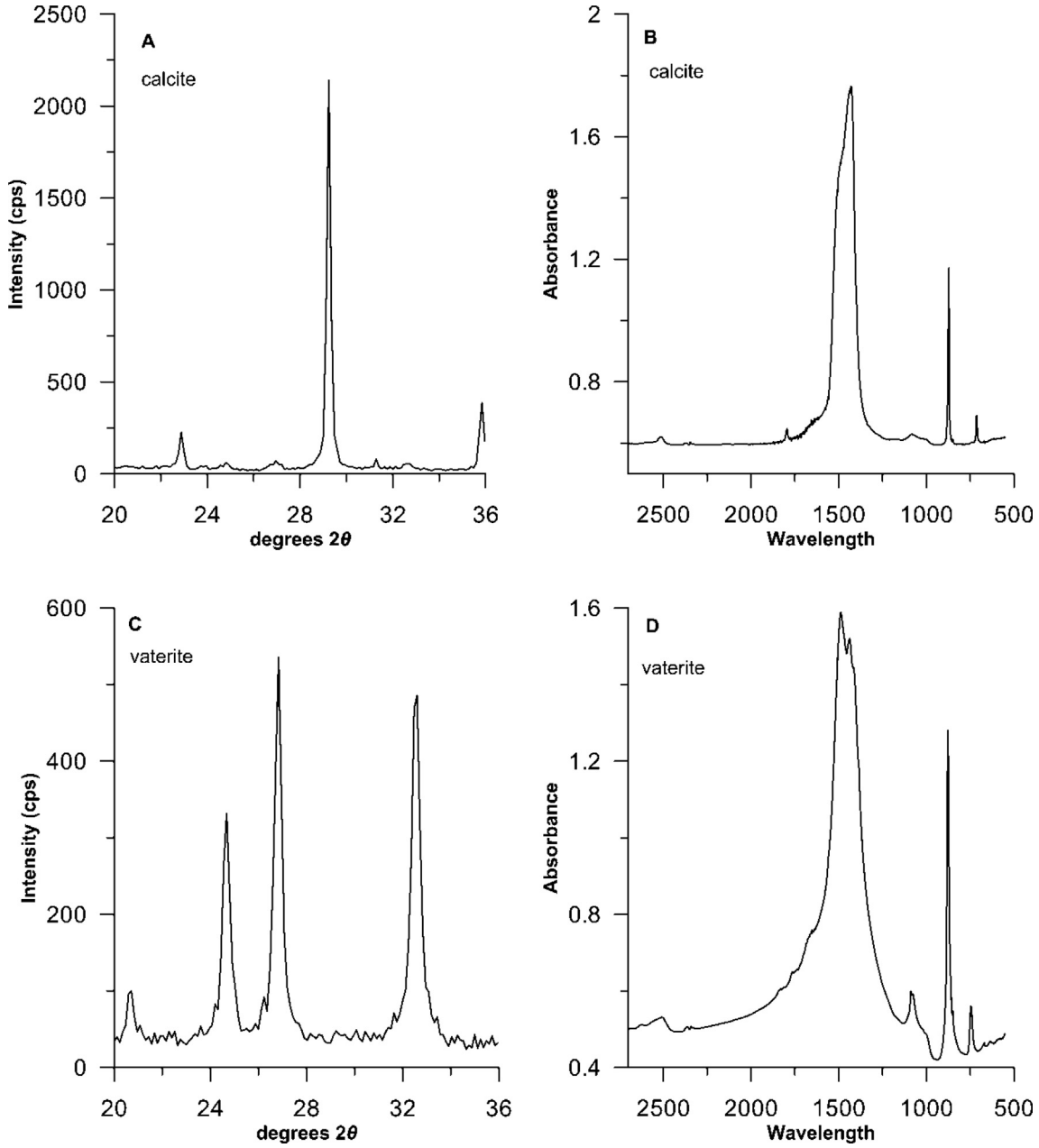

Fig. 2. XRD and FTIR spectra of calcite (A and B) and vaterite (C and D) identified in biomineralization experiments. Calcite peaks on FTIR are at 713, 875, 1423 (single), 1794 and 2516 cm^{-1}. Vaterite peaks are at 745, 875, 1084, 1437–1487 (double peak) and 2508 cm^{-1}. In XRD, the corresponding 2θ degrees for calcite were at 23.05 (9%), 29.40 (100%), and 35.96 (15%) and for vaterite were at 24.87 (90%), 27.01 (100%), and 32.80 (90%).

The morphological characteristics of the biomineral during the 30 °C experimental session are presented because this was the temperature that provided the optimum results (Fig. 3). Fig. 3a shows the blank marble surface at the end of the experiments. No apparent precipitation is obvious that could imply the inorganic formation of $CaCO_3$. Fig. 3b shows a sample from day 6 where bio-precipitation could be identified. A lower magnification is used in order to display both the substrate and vaterite. Biomineral particles, with spherical morphologies, dictate the new vaterite. Fig. 3c corresponds to day 9 where complete coverage of the surface was achieved. The cracks detected are observed in all the samples and may be due to the vacuum applied during scanning electron microscopy. However, the cracks did not pose any threat to the consistency of the biomineral, as will be discussed later. Fig. 3d–f show the vaterite morphology from day 9 to day 15 of the experiment, where complete substrate coverage was achieved. In Fig. 3d the black arrows indicate the biomineralized bacteria that are entangled with the micritic spheres, represented by the white arrows. While the bio-precipitation is ongoing, more biomineralized bacteria are deposited on the surface (Fig. 3e) and by the end of the experiment the microcrystalline spheres prevail, forming the final vaterite layer (Fig. 3f).

Weight loss with ultrasonic treatment and color measurements

The average weight loss percentage (Fig. 4) revealed a detectable consolidation effect of the new biomineral from 6 day samples. Better results were obtained for samples from day 9 to day 15. The day 15 samples provided slightly poorer consolidation results when compared with those of day 12. During sonication, the biomineral loosely attached onto the surface or marble fragments, where completely removed. The coherence of the vaterite layers is presented compared with the cleared marble surface (Fig. 5a), while the morphology remained unaltered (Fig. 5b).

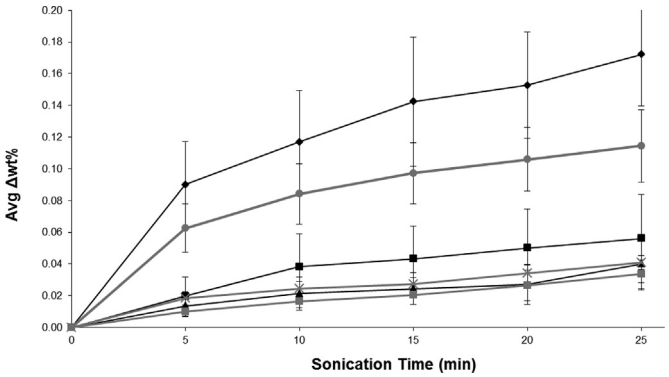

Fig. 4. Average weight loss percentage from marble samples during each sonication treatment. A detectable reduction in weight loss is shown for the samples from 6th to 15th experimental day. (◆) 3rd day samples; (●) blank; (■) 6th day samples; (▲) 9th day samples; (■) 12th day samples and (×) 15th day samples. Error bars: Standard Deviation.

Sonicated samples were cut into thin sections and analyzed. Fig. 6 shows the continuous vaterite layer that covered the marble. Regardless of the sonication treatment, thin section analysis did not reveal any significant fragmentation in the biomineral infrastructure. The new layer was compact and clearly distinguishable under the microscope following the anaglyph of the substrate (Fig. 6a). Cracks are attributed to sample preparation and are clearly visible in the electron photomicrographs of the thin sections (white arrow Fig. 6b) analyzed semi-quantitatively with EDS. The bio-consolidation efficiency of the bacterially induced vaterite is

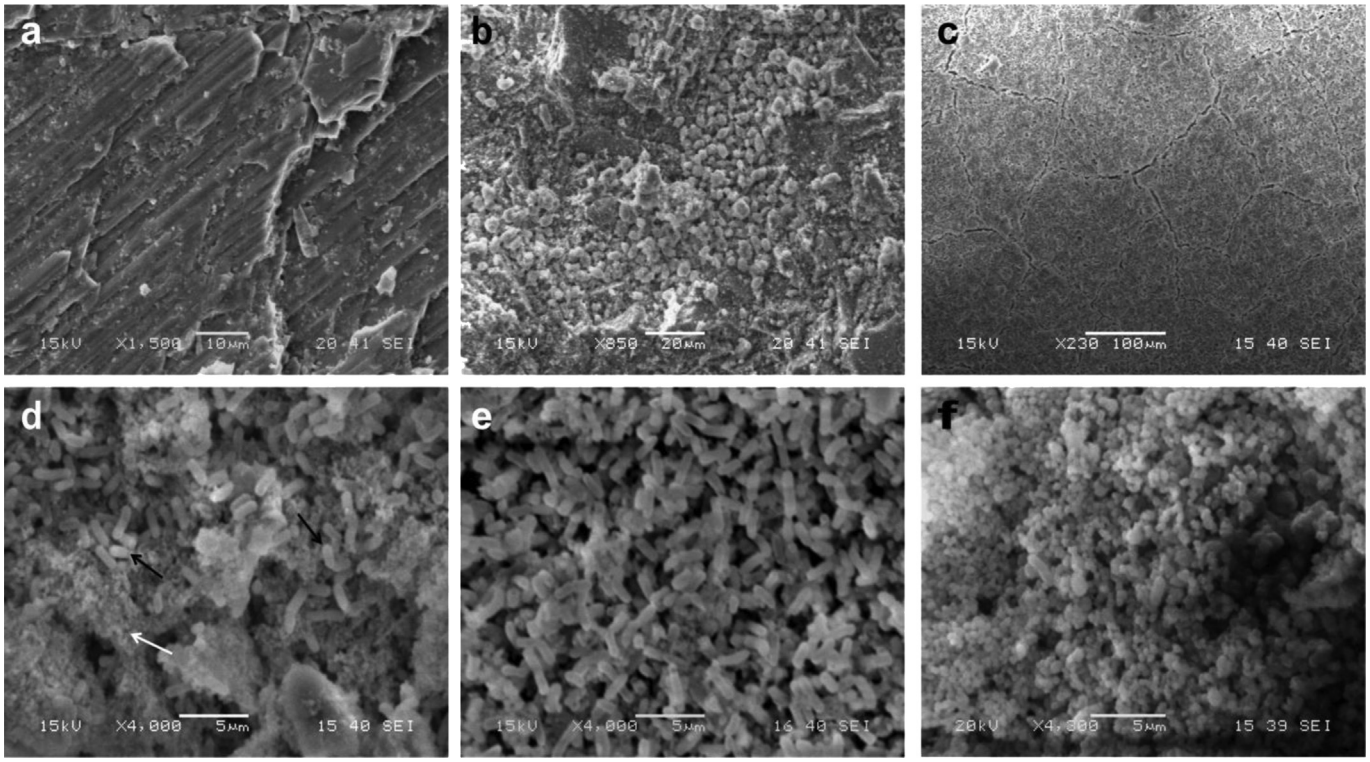

Fig. 3. Scanning electron microscopy of marble samples under optimum biomineralization conditions (30 °C). (a) Blank marble; (b) marble surface the 6th experimental day where initial biomineralization was identified; (c) complete coverage of the marble surface on 9th experimental day; (d) magnification of (c) where biomineralized cells (black arrows) and micritic spheres (white arrow) are the prevailing morphologies; (e) biomineral morphology on the 12th experimental day where biomineralized bacteria were mainly observed and (f) biomineral morphology on the final (15th) experimental day where both morphologies continue to contribute in precipitation but micritic spheres seem to prevail.

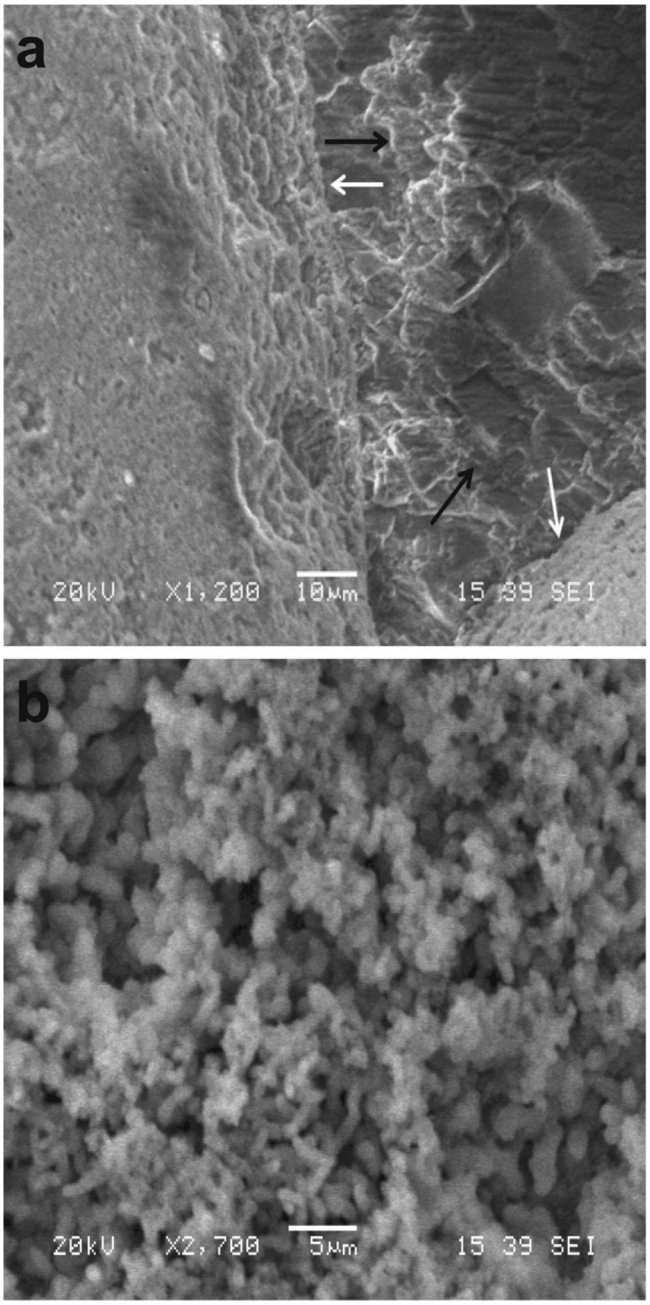

Fig. 5. Scanning electron photomicrographs. (a) Day 12 sample subjected to sonication treatment. The right side is the marble substrate (black arrows), with the left and lower right being the biomineral (white arrows). The photomicrograph is focused upon the surface of the substrate showing the difference in height and the consecutive layers of vaterite. Substrate's surface was completely cleared from loose material or marble fragments; (b) Magnification of the biomineral showing vaterite's preserved morphological characteristics after sonication.

presented by the filling up of the voids between the marble fragments (Fig. 6b white arrowheads). Semi-quantitative analysis of the left side of the sample (biomineral, Fig. 6b) could be distinguished from the substrate by trace amounts of phosphorus. The substrate did not show that peak (Suppl. Fig. 3).

After sonication, each sample was tested for its color differentiation. Control samples revealed no color differentiation. In samples where almost the entire surface was covered with vaterite, a distinct color difference in all the chromatic coordinates was visible (Table 3). $\mathbf{\Delta L^*}$ and $\mathbf{\Delta a^*}$ did not show considerable difference. Values in the $\mathbf{b^*}$ axis, yellow (positive) − blue (negative), showed a positive increase denoting more amounts of yellow color in the newly formed biomineral. Therefore, the $\mathbf{\Delta E}$ coordinates, representing the total color difference, are affected primarily by the differences in the $\mathbf{b^*}$ values. $\mathbf{\Delta E}$ exceed the limit of $\mathbf{\Delta E} \geq 3$ which is regarded as the difference detected by the naked eye. Most of the values, among the samples with a profound bio-consolidation effect, fall between $3.5 < \mathbf{\Delta E} < 6$ denoting a detectable difference.

Evaluation of the biodeposition treatment

Based on the data for acetate and calcium consumption under optimum conditions, the time span that each solution was applied for was 72–96 h, literally day 3 to day 4. Therefore, it was the onset of the acetate assimilation, calcium immobilization and bacterially induced precipitation that ensured that the results would be due to the ability of *B. pumilus* ACA-DC 4061 to promote biomineralization *in situ*. Concentration of the sprayed bacterial population was similar to the values achieved under optimum conditions. Fig. 7a shows a site with no obvious biomineralization, at the end of the treatment, while Fig. 7b presents a different area where the biomineralization occurred partially; bacteria first accumulated either wherever the marble crystals changed direction or in the surface cavities. Fig. 7c proves the presence of areas with a consistent new layer of biomineral covering the marble surface. Complete coverage was not achieved. Nonetheless, that can be accomplished by spraying a higher quantity of the bacterial solution. Fig. 7d–f present the morphology of the biomineral which proved to be analogous to sterile conditions: hollow hemispherical morphologies (Fig. 7d) where the cells "escaped" complete entombment from the $CaCO_3$ and biomineralized bacteria (Fig. 7e). Actual dimensions of both are revealed under high magnification (Fig. 7f). The color coordinates remained low (Table 3), mainly due to the fact that the samples were covered with less biomineral than those under sterile conditions.

Discussion

In this study we intended to investigate the mineralogy and morphology of calcium carbonate precipitation during the *B. pumilus* ACA-DC 4061 growth. Such an investigation could assist in determining whether the isolated strain could potentially be considered for the conservation intervention of stone monuments.

The Dionysus marble selected is a challenging substrate as it falls among the stones having the lowest porosity. The lack of pores does not provide readily accessible sites for microorganisms to colonize the substrate.

The growth medium implemented is of key importance for the biomineral outcome. Numerous media have been utilized with B4 medium suggested by Boquet et al. (1973), being the first option for the preliminary experiments (Marvasi et al., 2012). Based on that medium we redeveloped one with bacteriological peptone as the main component and different isolates were able to promote biomineralization (Daskalakis et al., 2013, 2014). *B. pumilus* ACA-DC 4061 was able to grow rapidly in this medium, as evident by its growth curve (Fig. S2). Furthermore, the pH could be adjusted to a value close to 8, thus reducing the incubation time for initiating biomineralization, while the microorganism further increased the pH of the solution during the experimental period. An alkaline environment is critical for successful biomineralization (De Muynck et al., 2010; Marvasi et al., 2012) promoted by bacterial metabolism.

Statistical analysis was investigated to assess whether it could predict the optimum biomineralization values for the parameters selected (temperature, growth medium and inoculum

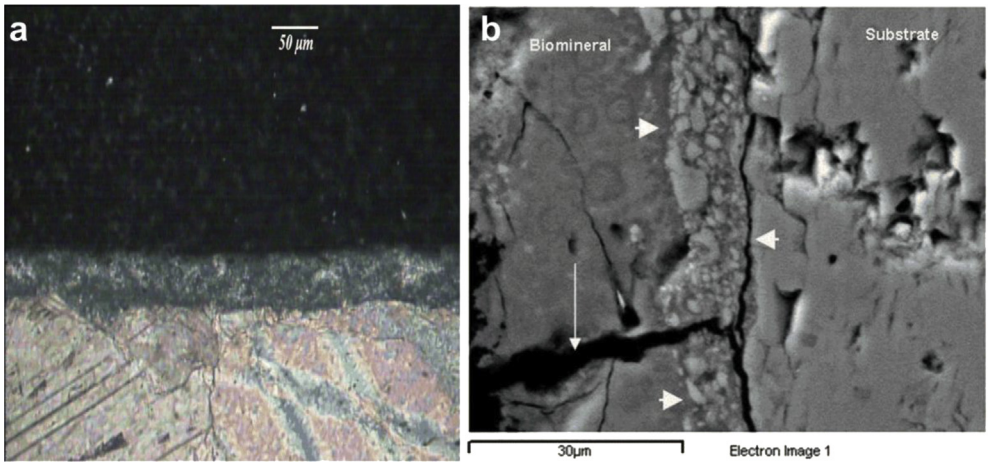

Fig. 6. Microscope analysis of thin sections of sonicated sample. (a) Sample after 12 days of incubation under the polarized microscope. The continuous biomineral layer is shown, following the anaglyph of the substrate; (b) same sample under the electron microscope. The left side of the picture presents the biomineral; the right side presents the marble substrate. Higher magnification shows that the novel material was detached as a whole due to forces exercised upon sample preparation, although the following of the anaglyph is still observable. The thin white arrow presents a perpendicular fissure of the biomineral. Marble fragments (white arrowheads) were consolidated with the novel vaterite layer.

concentration). The lowest temperature of 25 °C was actually among the values that showed high biomineralization efficiency. Nevertheless, experimental knowledge regarding the microorganism's optimum growth conditions dictated that 30 °C was the temperature at which the *B. pumilus* ACA-DC 4061 would show optimum growth. The raw data (not shown), from the series of experiments performed indicated that the highest biomineralization value resided among the 30 °C trials. Therefore, this temperature was also tested maintaining the rest of the parameters as identical. It was proven that 30 °C supported a stable nutrient assimilation that resulted in higher bio-precipitation (Fig. 1d). In a previous investigation of a Gram-negative microorganism (*C. metallidurans* ACA-DC 4073), a similar statistical design provided a set of parameters that was experimentally confirmed (Daskalakis et al., 2014). In the present study, all the sets of 15 trials per statistical experiment were performed simultaneously in order to avoid any bias between the different experimental days. The model obtained proved helpful in decreasing the experimental time necessary to investigate a wide range of different conditions. *B. pumilus* ACA-DC 4061 proved its ability to induce the $CaCO_3$ biomineralization within a specific range of temperatures and growth medium concentrations.

Table 3
Chromatic coordinates of sonicated marble substrates after the optimum-conditions experiment of *B. pumilus* ACA-DC 4061 biomineralization (3 day–15 day samples) and after the spraying application under non sterile conditions (No 1–No 4 samples).

Date of samples	Avg ΔL^{*}[a]	Avg Δa^{*}[a]	Avg Δb^{*}[a]	Avg ΔE^{*}
3-day marbles	0.06	0.13	0.04	0.22
6-day marbles	−1.31	−0.05	2.19	2.66
9-day marbles	−2.13	−0.28	3.15	4.09
12-day marbles	−1.42	−0.38	4.69	4.96
15-day marbles	−1.05	−0.65	6.22	6.37
Control marble	L^{*}[b]	a^{*}[b]	b^{*}[b]	
	90.56	−0.85	−1.37	
Sample No	ΔL^{*}[c]	Δa^{*}[c]	Δb^{*}[c]	ΔE^{*}
1	0.69	−0.48	1.51	1.79
2	0.63	−0.63	2.83	2.97
3	1.26	−0.54	2.95	3.25
4	2.57	−0.39	2.77	3.80
Control marble	L^{*}[b]	a^{*}[b]	b^{*}[b]	
	84.98	−0.9	−1.99	

[a] Values correspond to the average from 3 samples for each experimental day. For each one of the 3 samples, 5 measurements were taken from different surface positions and the average value was calculated from the instrument's software.
[b] For control marble, the actual values are presented for comparison purposes.
[c] For the experiments under non sterile conditions for each numbered sample the average of 5 measurements from the substrate's surface are presented as calculated from the instrument's software.

Acetate considerably assisted in the biomineralization process by increasing the cell population via diauxic growth. Cell concentration proved critical under the experimental conditions investigated. A higher utilization of acetate and cell concentration should cause a higher immobilization of calcium and eventually a faster biomineralization rate. However, the opposite was documented: *B. pumilus* ACA-DC 4061 at 25 °C, despite the overall faster acetate utilization and higher cell concentration, it produced less biomineral compared to 30 °C. According to the vaterite morphology, the biomineralization of cells was the main morphology of the bio-precipitate. At 30 °C, lower cell concentration and their concurrent biomineralization provided a steady formation of vaterite on the marble. At 25 °C, the increased cell concentration caused higher calcium dispersion on the live cells and possibly its concentration was insufficient to biomineralize the whole cells.

Calcium was practically exhausted until the 12th experimental day, while there was still a portion of acetate that remained unutilized. Such nutrient conditions may explain the slight difference in the final vaterite morphology identified on the substrates. Spherical vaterite seems to prevail at the end of the experiment (Fig. 3f) when compared with the rod-shaped vaterite observed on the samples from day 12 of the experiment (Fig 3e). The quantity of calcium is insufficient to biomineralize all cells, while their metabolism promoted the micritic sphere formation in close vicinity of the cells. Nevertheless, biomineralized bacteria continued to be identified among the spheres.

In our experiments the consistency of vaterite formation is noteworthy. Vaterite is the least stable among the three anhydrous polymorphs of calcium carbonate and transforms to the most stable calcite under ambient conditions of temperature and pressure (Suzuki et al., 2006). This holds true during inorganic precipitation. When the organic molecules and biomolecules enter into the process, the stability of the vaterite gets improved.

Stearic acid monolayers (Mann et al., 1988) and phospholipid monolayers (Xiao et al., 2009) stabilize the vaterite. Amino acids

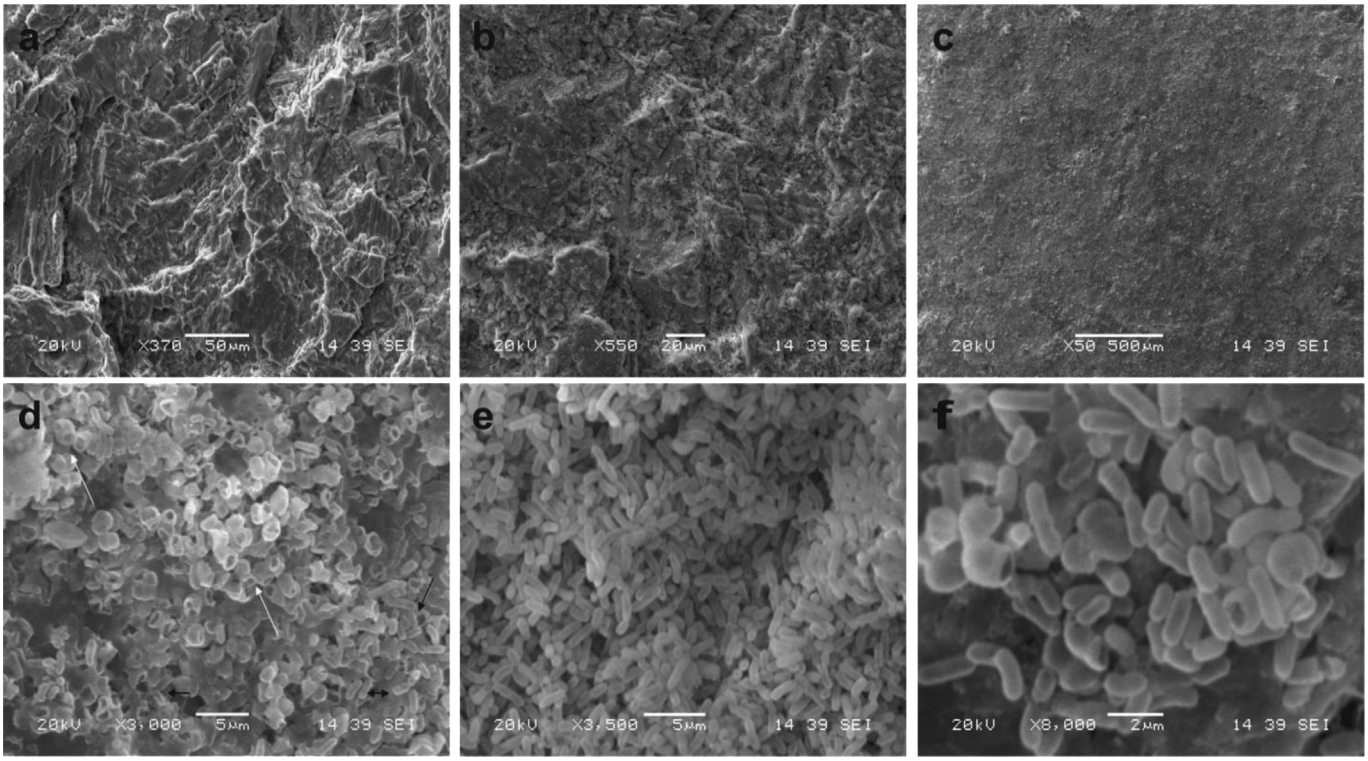

Fig. 7. Panoramic view of marble after 10-day spraying period: (a) An area of no coverage from the new biomineral; (b) an area of low coverage from the new biomineral and (c) an area of high coverage from the new biomineral. Biomineral morphology: (d) Magnification presenting the prevailing morphologies with biomineralized bacteria (black arrows) and hollow hemispheres where bacterial cells were not completely covered from calcium carbonate; (e) a different site where biomineralized cell rods covered the marble surface and (f) maximum magnification achieved under the electron microscope presenting the actual size of biomineralized cells and hemispheres.

may exert control in the calcium carbonate polymorphism under specific experimental conditions (Manoli and Dalas, 2001; Li et al., 2002; Malkaj et al., 2004; Malkaj and Dalas, 2004; Xie et al., 2005; Wolf et al., 2007). Polysaccharides and their components, improve the vaterite stability (Natoli et al., 2010) whereas the phosphate ions delay its transformation to calcite (Katsifaras and Spanos, 1999). Chitosan, shown to induce vaterite formation (Wu et al., 2011), contains N-acetyl-D-glucosamine which is encountered as a component of the Gram positive bacterial cell walls.

Gram-positive bacterial cell walls could include the characteristics mentioned above due to their components. Peptidoglycans, teichoic and lipoteichoic acids provide the cell wall with negative charge. The concentration of the phosphate groups versus D-alanyl esters in teichoic and lipoteichoic acids play a crucial role in the overall negative charge of the bacterial cell wall (Neuhaus and Baddiley, 2003; Vollmer et al., 2008; Potekhina et al., 2011). Free carboxyl groups inside the peptide stem that connects the glycan strands can further assist in this function, while bacterial growth and cell health will tailor the overall effect of these moieties (Neuhaus and Baddiley, 2003). Furthermore, the proteins anchored on the cell wall could provide additional positive or negative sites for carbonate and calcium coordination.

Calcite formed when *Sporosarcina pasteurii* (former *Bacillus pasteurii*) (Bang et al., 2001; Mitchell and Ferris, 2006) or other ureolytic bacteria were tested (Fujita et al., 2000) Similarly, *B. sphaericus* stabilized the calcite in solid media (Hammes et al., 2003) and when limestone was immersed in the liquid growth medium (Dick et al., 2006). On the contrary, when the nutrient broth and calcium acetate were substituted with calcium chloride, vaterite with a spherical morphology was identified for both *B. sphaericus* (De Muynck et al., 2008a) and *S. pasteurii* (Kim et al., 2013). The growth medium we implemented had a lower calcium acetate concentration (0.05 M) compared with the one used by De Muynck et al. (2008a) (0.32 M) and Kim et al. (2013) (0.16 M). Assuming that vaterite formation could be formed when similar nutrients are used among the *Bacillus* isolates, then the calcium acetate concentration presented in this work may reside to the low limit for vaterite formation. As mentioned in the Results Section, vaterite was consistently detected in BP3x concentration. Recently *Lysinibacillus sphaericus* (former *B. sphaericus*) produced vaterite in a modified B4 medium (Shirakawa et al., 2011). Nutrient surplus (due to nutrient broth and acetate) induced biomineralization while the biomolecules stabilized the vaterite formation.

If the vaterite crystals were temporal or of inorganic origin we should have been able to notice a gradual transformation to calcite via the solid state transition and/or solution mediated transformation (Li et al., 2002) or after sonication treatment (Berdonosov et al., 2005). The FT-IR and XRD spectra of the calcium carbonate crystals stored under ambient conditions and analyzed a year later, did not show any difference; thus the solid–state transition did not occur. Redissolution and gradual evaporation of the samples confirmed the stability of the vaterite; thus, solution-mediated transformation to calcite did not occur either. These results prove the stability of vaterite and the fact that the Ostwald's rule of stages was interrupted. Vaterite is formed first as the less stable polymorph (highest solubility) and its transformation is inhibited by the incorporation of the organic components (Li et al., 2002). Therefore, the main morphology mimicked bacterial dimensions. The presence of the spherical vaterite, smaller than bacterial dimensions, but in direct contact with them, may be considered the “precursor” morphology created upon the bacterial cell membrane with the bacterial encapsulation remaining

unfinished. Alternatively, the bacterial macromolecules, released from the cells or due to their death, may result in such vaterite micritic spheres.

Rodriguez-Navarro et al. (2003) suggested the ultrasonic treatment of the samples as an estimate of the adhesion force and consolidation efficacy of the new biomineral. Blank samples obtained after the experiments and subjected to sonication, were completely cleared from any loosely attached material and marble fragments (Fig. 5a). The Δwt% of the blank samples vs the biomineralized samples was reduced as the latter showed the stability of the vaterite on the marble surface. A similar effect was reported for *B. sphaericus* (De Muynck et al., 2010). The values presented here are lower due to the negligible porosity of marble. The biomineral resided only on the marble surface and not inside the pores of a limestone. That would have increased the biomineral deposition as dictated from our preliminary experiments conducted on porous limestone (results not shown). The biomineral deposited within the pore network would be "protected" from sonication forces. Stability was further validated from the continuous vaterite layer visible in the thin section analysis of the sonicated samples. Scanning electron microscopy (Fig. 6b) proved that even marble fragments were fixed onto the surface as a result of the biomineralization. Finally, the morphological characteristics remained unaltered based on scanning electron microscopy. The biologically induced mineralization of vaterite was further supported by the phosphorus peak observed. No such peak was observed in any control sample. Its low percentage values demonstrated that it could be of biological origin and not due to the formation of a different biomineral. A similar peak was observed in the samples during the evaluation of *C. metallidurans* ACA-DC 4073 (Daskalakis et al., 2014). Marvasi et al., 2012, have also reported the presence of a phosphorus peak in the $CaCO_3$ samples from isolated bacteria. Finally, the FT-IR analysis of the sample did not show any differentiation, negating the possibility of a different biomineral.

The color effect of the new material remained at its minimum and only the last set of samples in the sterile experiment recorded $\Delta E > 6$, a value that is considered unacceptable during monument interventions. Therefore, under optimum growth conditions, *B. pumilus* ACA-DC 4061 promotes a newly formed biomineral that does not considerably affect the substrate color. In the non-sterile experiment, where the volume of the nutrient-bacterial solution was minimal, the color differentiation was observed to be even lower. This may be an advantageous characteristic of the microorganism because it can be applied in greater volumes and provide a more pronounced bioconsolidation effect in a real case scenario, with reduced color differentiation. Its maximum weight increase was almost twice as much compared with *C. metallidurans* ACA-DC 4073; while the ΔE was considerably lower, slightly above the value of $\Delta E \leq 6$ compared with our Gram-negative isolate (Daskalakis et al., 2014).

A scaled-up experiment was performed in order to observe the biomineralization efficiency of *B. pumilus* ACA-DC 4061 under conditions relatively closer to that of the environment. Non sterile conditions were adopted to investigate the potential of antagonistic growth of other microorganisms during application. No obvious contamination was detected showing that the selected microorganism was the main recipient of the nutrients. High humidity, to delay the drying of the substrate was performed for two reasons: to avoid the potential of spore formation of the applied microorganism, which could delay the biomineralization and to assist growth of other microorganisms. Temperature was kept constant as the first step in this experimental series while in future tests temperature will not be controlled. The biomineral mainly possessed bacterial cell dimensions suggesting that the process was performed primarily upon the cells or close to them, excluding inorganic precipitation. . Spraying the minimum quantity of bacterial solution on the marble revealed that the morphology corresponded to vaterite. The calcium carbonate polymorph proved stable even under those conditions.

The question that may arise is whether vaterite is bacterial or nutrient specific. Bacterial isolates identified having the ability to produce vaterite are constantly increasing. They belong to different genera and have been isolated from different environmental niches. If we combine the results of *B. pumilus* ACA-DC 4061 and *B. sphaericus* (De Muynck et al., 2008a, b; Shirakawa et al., 2011) we can hypothesize that the main cause is the nutrient content provided. Both isolates promoted vaterite in a more nutritious environment and on different substrates. A *Bacillus* isolate promoted vaterite and calcite mixtures when M3P medium was applied on stone (Jroundi et al., 2010). On extending to Gram − negative isolates such as *C. metallidurans* ACA-DC 4073 (with BP3x medium), *Pantoea* spp., *Pseudomonas chlororaphis* (BP2x and BP4x medium) (Daskalakis et al., 2013) and *Myxococxus xanthus* (M-3 medium) (Jimenez-Lopez et al., 2007) vaterite was identified. In all the cases cited above the main similarity is calcium acetate: acetate promotes better growth of the bacteria implemented and the faster metabolism could stabilize the vaterite, as described in this work. Both types of cell membranes possess the components necessary for stabilizing the $CaCO_3$ and the type of nutrient that will boost bacterial growth may be the key factor to the prevalence and stability of the vaterite.

Conclusion

We investigated the ability of *B. pumilus* ACA-DC 4061 to promote biomineralization of calcium carbonate under specific growth conditions, obtained from the statistical analysis of three main factors: temperature, medium and inoculum concentration. We identified a constant formation of stable vaterite even in samples re-evaluated after a year. Biomineralization tests on the marble samples resembling *in situ* conditions showed similar morphologies. Thus we may summarize that vaterite, under the conditions presented, provided detectable biomineralization on a stone substrate. Further proof should be obtained that will demonstrate a long-term stability and the results presented in this study combined with the observations of other research groups are the first step towards it. Validation on bigger stone samples, in outdoor environmental conditions and additional mechanical tests would provide further insight on *B. pumilus* ACA-DC 4061 potential. Furthermore, we may regard its morphological differentiation as an advantage which will assist in the biomineral assessment on stone and its distinctiveness from the substrate. Such a characteristic could assist in the monitoring of the *in situ* applications for the bioconsolidation impact of vaterite and its endurance under various environmental and chemical factors.

Acknowledgment

This work was supported by the Ministry of National Education and Religious Affairs (Community Support Framework, 2000–2006) under the Pythagoras II Research Program (Project No. 68/751). The Project is co-funded by the European Social Fund (75%) and National Resources (25%).

Appendix A. Supplementary data

Supplementary data related to this article can be found at http://dx.doi.org/10.1016/j.ibiod.2014.12.005.

References

Achal, V., Mukherjee, A., Basu, P.C., Sudhakara Reddy, M., 2009. Strain improvement of *Sporosarcina pasteurii* for enhanced urease and calcite production. J. Ind. Microbiol. Biotechnol. 36, 981–988. http://dx.doi.org/10.1007/s10295-009-0578-z.

Achal, V., Mukherjee, A., Sudhakara Reddy, M., 2013. Biogenic treatment improves the durability and remediates the cracks of concrete structures. Constr. Build. Mater. 48, 1–5. http://dx.doi.org/10.1016/j.conbuildmat.2013.06.061.

Adolphe, J.-P., Loubière, J.-F., Paradas, J., Soleilhavoup, F., 1990. Procédé de traitement biologique d' une surface artificielle. European patent No. 90400697.0 (after French patent No. 8903517, 1989).

Anne, S., Rozenbaum, O., Andreazza, P., Rouet, J.-L., 2010. Evidence of a bacterial carbonate coating on plaster samples subjected to the Calcite Bioconcept biomineralization technique. Constr. Build. Mater. 24, 1036–1042. http://dx.doi.org/10.1016/j.conbuildmat.2009.11.014.

Bang, S.S., Galinat, J.K., Ramakrishnan, V., 2001. Calcite precipitation induced by polyurethane-immobilized *Bacillus pasteurii*. Enzyme Microb. Technol. 28, 404–409. http://dx.doi.org/10.1016/S0141-0229(00)00348-3.

Barton, H.A., Northup, D.E., 2007. Geomicrobiology in cave environments: past, current and future perspectives. J. Cave Karst Stud. 69, 163–178.

Baskar, S., Baskar, R., Mauclaire, L., McKenzie, J.A., 2006. Microbially induced calcite precipitation in culture experiments: possible origin for stalactites in Sahastradhara caves, Dehradun, India. Curr. Sci. 90, 58–64.

Berdonosov, S.S., Znamenskaya, I.V., Melikhov, I.V., 2005. Mechanism of the vaterite-to-calcite phase transition under sonication. Inorg. Mater. 41, 1308–1312. http://dx.doi.org/10.1007/s10789-005-0307-6.

Boquet, E., Boronat, A., Ramos-Comerzana, A., 1973. Production of calcite (calcium carbonate) crystals by soil bacteria is a general phenomenon. Nature 246, 527–529. http://dx.doi.org/10.1038/246527a0.

Cacchio, P., Ercole, C., Cappuccio, G., Lepidi, A., 2003. Calcium carbonate precipitation by bacterial strains isolated from a limestone cave and from a loamy soil. Geomicrobiol. J. 20, 85–98. http://dx.doi.org/10.1080/01490450303883.

Castanier, S., Le Métayer-Levrel, G., Orial, G., Loubière, J.-F., Perthuisot, J.-P., 2000. Bacterial carbonatogenesis and applications to preservation and restoration of historic property. In: Ciferri, O., Tiano, P., Mastromei, G. (Eds.), Of Microbes and Art: the Role of Microbial Communities in the Degradation and Protection of Cultural Heritage. Proceedings of an International Conference on Microbiology and Conservation, Florence, Italy. Kluwer Academic/Plenum Publishers, New York, pp. 203–218.

ChunXiang, Q., QingFeng, P., Ruiing, W., 2010. Cementation of sand grains based on carbonate precipitation induced by microorganism. Sci. China Technol. Sci. 53, 2198–2206. http://dx.doi.org/10.1007/s11431-009-3189-z.

Daskalakis, M.I., Magoulas, A., Kotoulas, G., Catsikis, I., Bakolas, A., Karageorgis, A.P., Mavridou, A., Doulia, D., Rigas, F., 2013. *Pseudomonas, Pantoea* and *Cupriavidus* isolates induce calcium carbonate precipitation for biorestoration of ornamental stone. J. Appl. Microbiol. 115, 409–423. http://dx.doi.org/10.1111/jam.12234.

Daskalakis, M.I., Magoulas, A., Kotoulas, G., Katsikis, I., Bakolas, A., Karageorgis, A.P., Mavridou, A., Doulia, D., Rigas, F., 2014. *Cupriavidus metallidurans* biomineralization ability and its application as a bioconsolidation enhancer for ornamental marble stone. Appl. Microbiol. Biotechnol. 98, 6871–6883. http://dx.doi.org/10.1007/s00253-014-5753-0.

De Muynck, W., Cox, K., De Belie, N., Verstraete, W., 2008a. Bacterial carbonate precipitation as an alternative surface treatment for concrete. Constr. Build. Mater. 22, 875–885. http://dx.doi.org/10.1016/j.conbuildmat.2006.12.011.

De Muynck, W., Debrouwer, D., De Belie, N., Verstraete, W., 2008b. Bacterial carbonate precipitation improves the durability of cementitious materials. Cem. Concr. Res. 38, 1005–1014. http://dx.doi.org/10.1016/j.cemconres.2008.03.005.

De Muynck, W., Verbeken, K., De Belie, N., Verstraete, W., 2010. Influence of urea and calcium dosage on the effectiveness of bacterially induced carbonate precipitation on limestone. Ecol. Eng. 36, 99–111. http://dx.doi.org/10.1016/j.ecoleng.2009.03.025.

De Muynck, W., Verbeken, K., De Belie, N., Vestraete, W., 2013. Influence of temperature on the effectiveness of a biogenic carbonate surface treatment for limestone conservation. Appl. Microbiol. Biotechnol. 97, 1335–1347. http://dx.doi.org/10.1007/s00253-012-3997-0.

DeJong, J.T., Mortensen, B.M., Martinez, B.C., Nelson, D.C., 2010. Bio-mediated soil improvement. Ecol. Eng. 36, 197–210. http://dx.doi.org/10.1016/j.ecoleng.2008.12.029.

Dick, J., De Windt, W., De Graef, B., Saveyn, H., Van der Meeren, P., De Belie, N., Verstraete, W., 2006. Bio-deposition of a calcium carbonate layer on degraded limestone by *Bacillus* species. Biodegradation 17, 357–367. http://dx.doi.org/10.1007/s10532-005-9006-x.

Douglas, S., 2005. Mineralogical footprints of microbial life. Am. J. Sci. 305, 503–525. http://dx.doi.org/10.2475/ajs.305.6-8.503.

Ettenauer, J., Piñar, G., Sterflinger, K., Gonzalez-Muñoz, M.T., Jroundi, F., 2011. Molecular monitoring of the microbial dynamics occurring on historical limestone buildings during and after the *in situ* application of different bio-consolidation treatments. Sci. Total Environ. 409, 5337–5352. http://dx.doi.org/10.1016/j.scitotenv.2011.08.063.

Fujita, Y., Ferris, F.G., Lawson, R.D., Colwell, F.S., Smith, R.W., 2000. Calcium carbonate precipitation by ureolytic subsurface bacteria. Geomicrobiol. J. 17, 305–318. http://dx.doi.org/10.1080/782198884.

Gadd, G.F., 2010. Metals, minerals and microbes: geomicrobiology and bioremediation. Microbiology 156, 609–643. http://dx.doi.org/10.1099/mic.0.037143-0.

Hammes, F., Boon, N., de Villiers, J., Verstraete, W., Siciliano, S.D., 2003. Strain-specific ureolytic microbial calcium carbonate precipitation. Appl. Environ. Microbiol. 69, 4901–4909. http://dx.doi.org/10.1128/AEM.69.8.4901-4909.2003.

Han, J., Lian, B., Ling, H., 2013. Induction of calcium carbonate by *Bacillus cereus*. Geomicrobiol. J. 30, 682–689. http://dx.doi.org/10.1080/01490451.2012.758194.

Jimenez-Lopez, C., Rodriguez-Navarro, C., Pinar, G., Carrillo-Rosúa, F.J., Rodriguez-Gallego, M., González-Muñoz, M.T., 2007. Consolidation of degraded ornamental porous limestone stone by calcium carbonate precipitation induced by the microbiota inhabiting the stone. Chemosphere 68, 1929–1936. http://dx.doi.org/10.1016/j.chemosphere.2007.02.044.

Jonkers, H.M., Thijssen, A., Muyzer, G., Copuroglu, O., Schlangen, E., 2010. Application of bacteria as self-healing agent for the development of sustainable concrete. Ecol. Eng. 36, 230–235. http://dx.doi.org/10.1016/j.ecoleng.2008.12.036.

Jroundi, F., Fernandez-Vivas, M.A., Rodriguez-Navarro, C., Bedmar, E.J., González-Muñoz, M.T., 2010. Bioconservation of deteriorated monumental calcarenite stone and identification of bacteria with carbonatogenic activity. Microbiol. Ecol. 60, 39–54. http://dx.doi.org/10.1007/s00248-010-9665-y.

Jroundi, F., Suaga-Gómez, P., Jimenez-Lopez, C., Gonzalez-Muñoz, M.T., Fernandez-Vivas, M.A., 2012. Stone-isolated carbonatogenic bacteria as inoculants in bioconsolidation treatments for historical limestone. Sci. Total Environ. 425, 89–98. http://dx.doi.org/10.1016/j.scitotenv.2012.02.059.

Katsifaras, A., Spanos, N., 1999. Effect of inorganic phosphate ions on the spontaneous precipitation of vaterite and on the transformation of vaterite to calcite. J. Cryst. Growth 204, 183–190. http://dx.doi.org/10.1016/S0022-0248(99)00174-8.

Kim, H.K., Park, S.J., Han, J.I., Lee, H.K., 2013. Microbially mediated calcium carbonate precipitation on normal and lightweight concrete. Constr. Build. Mater. 38, 1073–1082. http://dx.doi.org/10.1016/j.conbuildmat.2012.07.040.

Lee, S.-W., Park, S.-B., Jeong, S.-K., Lim, K.-S., Lee, S.-H., Trachtenberg, M.C., 2010. On carbon dioxide storage based on biomineralization strategies. Micron 41, 273–282. http://dx.doi.org/10.1016/j.micron.2009.11.012.

Li, C., Botsaris, G.D., Kaplan, D.L., 2002. Selective in vitro effect of peptides on calcium carbonate crystallization. Cryst. Growth Des. 2, 387–393. http://dx.doi.org/10.1021/cg0255467.

Lovett, P.S., Young, F.E., 1969. Identification of *Bacillus subtilis* NRRL B-3275 as a strain of *Bacillus pumilus*. J. Bacteriol. 100, 658–661.

Malkaj, P., Dalas, E., 2004. Calcium carbonate crystallization in the presence of aspartic acid. Cryst. Growth Des. 4, 721–723. http://dx.doi.org/10.1021/cg030014r.

Malkaj, P., Kanakis, J., Dalas, E., 2004. The effect of leucine on the crystal growth of calcium carbonate. J. Cryst. Growth 266, 533–538. http://dx.doi.org/10.1016/j.jcrysgro.2004.02.114.

Mann, S., Heywood, B.R., Rajam, S., Birchall, J.D., 1988. Controlled crystallization of $CaCO_3$ under stearic acid monolayers. Nature 334, 692–695. http://dx.doi.org/10.1038/334692a0.

Manoli, F., Dalas, E., 2001. Calcium carbonate crystallization in the presence of glutamic acid. J. Cryst. Growth 222, 293–297. http://dx.doi.org/10.1016/S0022-0248(00)00893-9.

Marvasi, M., Gallagher, K.L., Martinez, L.C., Pagan, W.C.M., Santiago, R.E.R., Vega, G.C., Visscher, P.T., 2012. Importance of B4 medium in determining organomineralization potential of bacterial environmental isolates. Geomicrobiol. J. 29, 916–924. http://dx.doi.org/10.1080/01490451.2011.636145.

Mitchell, A.C., Ferris, F.G., 2006. The influence of *Bacillus pasteurii* on the nucleation and growth of calcium carbonate. Geomicrobiol. J. 23, 213–226. http://dx.doi.org/10.1080/01490450600724233.

Natoli, A., Wiens, M., Schröder, H.-C., Stifanic, M., Batel, R., Soldati, A.L., Jacob, D.E., Müller, W.E.G., 2010. Bio-vaterite formation by glycoproteins from freshwater pearls. Micron 41, 359–366. http://dx.doi.org/10.1016/j.micron.2010.01.002.

Neuhaus, F.C., Baddiley, J., 2003. A continuum of anionic charge: structures and function of D-alanyl-teichoic acids in gram-positive bacteria. Microbiol. Mol. Biol. Rev. 67, 686–723. http://dx.doi.org/10.1128/MMBR.67.4.686-723.2003.

O'Donnell, A.G., Norris, J.R., Berkeley, R.C.W., Claus, D., Kaneko, T., Logan, N.A., Nozaki, R., 1980. Characterizations of *Bacillus subtilis*, *Bacillus pumilus*, *Bacillus licheniformis*, and *Bacillus amyloliquefaciens* by pyrolysis gas-liquid chromatography, deoxyribonucleic acid- deoxyribonucleic acid hybridization, biochemical tests and API systems. Int. J. Syst. Bacteriol. 30, 448–459. http://dx.doi.org/10.1099/00207713-30-2-448.

Pecher, J., Guenoun, P., Chevallard, C., 2009. Crystalline calcium carbonate thin film formation through interfacial growth and crystallization of amorphous microdomains. Cryst. Growth Des. 9, 1306–1311. http://dx.doi.org/10.1021/cg800251t.

Piñar, G., Jimenez-Lopez, C., Sterflinger, K., Ettenauer, J., Jroundi, F., Fernandez-Vivas, A., Gonzalez-Muñoz, M.T., 2010. Bacterial community dynamics during the application of a *Myxococxus xanthus*-inoculated culture medium used for consolidation of ornamental limestone. Microbiol. Ecol. 60, 15–28. http://dx.doi.org/10.1007/s00248-010-9661-2.

Pope, G.A., Meierding, T.C., Paradise, T.R., 2002. Geomorphology's role in the study of weathering of cultural stone. Geomorphology 47, 211–225. http://dx.doi.org/10.1016/S0169-555X(02)00098-3.

Potekhina, N.V., Streshinskaya, G.M., Tulskaya, E.M., Kozlova, Yu I., Senchenkova, S.N., Shashkov, A.S., 2011. Phosphate – containing cell wall polymers of bacilli. Biochemistry (Moscow) 76, 745–754. http://dx.doi.org/10.1134/S0006297911070042.

Priest, F.G., Goodfellow, M., Todd, C., 1988. A numerical classification of the genus *Bacillus*. J. General Microbiol. 134, 1847–1882. http://dx.doi.org/10.1099/00221287-134-7-1847.

Ramachandran, S.K., Ramakrishnan, V., Bang, S.S., 2001. Remediation of concrete using micro-organisms. ACI Mater. J. 98, 3–9. http://dx.doi.org/10.14359/10154.

Rodriguez-Navarro, C., Rodriguez-Gallego, M., Chekroun, K.B., Gonzalez-Munoz, M.T., 2003. Conservation of ornamental stone by *Myxococcus xanthus* – induced carbonate biomineralization. Appl. Environ. Microbiol. 64, 2182–2193. http://dx.doi.org/10.1128/AEM.69.4.2182-2193.2003.

Sarda, D., Choonia, H.S., Sarode, D.D., Lele, S.S., 2009. Biocalcification by *Bacillus pasteurii* urease: a novel application. J. Ind. Microbiol. Biotechnol. 36, 1111–1115. http://dx.doi.org/10.1007/s10295-009-0581-4.

Scheerer, S., Ortega-Morales, O., Gaylarde, C., 2009. Microbial deterioration of stone monuments – an updated overview. Adv. Appl. Microbiol. 66, 97–139. http://dx.doi.org/10.1016/S0065-2164(08)00805-8.

Shirakawa, M.A., Cincotto, M.A., Atencio, D., Gaylarde, C.C., Vanderley, M.J., 2011. Effect of culture medium on biocalcification by *Pseudomonas putida, Lysinibacillus sphaericus* and *Bacillus subtilis*. Braz. J. Microbiol. 42, 499–507. http://dx.doi.org/10.1590/S1517-838220110002000014.

Smith, B.J., Gomez-Heras, M., McCabe, S., 2008. Understanding the decay of stone-built cultural heritage. Prog. Phys. Geogr. 32, 439–461. http://dx.doi.org/10.1177/0309133308098119.

Stocks-Fischer, S., Galinat, J.K., Bang, S.S., 1999. Microbiological precipitation of $CaCO_3$. Soil Biology and Biochemistry 31, 1563–1571. http://dx.doi.org/10.1016/S0038-0717(99)00082-6.

Suzuki, M., Nagasawa, H., Kogure, T., 2006. Synthesis and structure of hollow calcite particles. Cryst. Growth Des. 6, 2004–2006. http://dx.doi.org/10.1021/cg0602921.

Vollmer, W., Blanot, D., De Pedro, M.A., 2008. Peptidoglycan structure and architecture. FEMS Microbiol. Rev. 32, 149–167. http://dx.doi.org/10.1111/j.1574-6976.2007.00094.x.

Warscheid, Th, Braams, J., 2000. Biodeterioration of stone: a review. Int. Biodeterior. Biodegrad. 46, 343–368. http://dx.doi.org/10.1016/S0964-8305(00)00109-8.

Wiktor, V., Jonkers, H.M., 2011. Quantification of crack-healing in novel bacteria-based self-healing concrete. Cem. Concr. Compos. 33, 763–770. http://dx.doi.org/10.1016/j.cemconcomp.2011.03.012.

Wolf, A.E., Loges, N., Mathiasch, B., Panthöfer, B., Mey, I., Janshoff, A., Tremel, W., 2007. Phase selection of calcium carbonate through the chirality of adsorbed amino acids. Angew. Chem. Int. Ed. 46, 5618–5623. http://dx.doi.org/10.1002/anie.200700010.

Wu, Y., Cheng, C., Yao, J., Chen, X., Shao, Z., 2011. Crystallization of calcium carbonate on chitosan substrates in the presence of regenerated silk fibroin. Langmuir 27, 2804–2810. http://dx.doi.org/10.1021/la104712h.

Xiao, J., Wang, Z., Tang, Y., Tang, S., 2009. Biomimetic mineralization of $CaCO_3$ on a phospholipid monolayer: from an amorphous calcium carbonate precursor to calcite via vaterite. Langmuir 26, 4977–4983. http://dx.doi.org/10.1021/la903641k.

Xie, A.-J., Shen, Y.-H., Zhang, C.-Y., Yuan, Z.-W., Zhu, X.-M., Yang, Y.-M., 2005. Crystal growth of calcium carbonate with various morphologies in different amino acid systems. J. Cryst. Growth 285, 436–443. http://dx.doi.org/10.1016/j.jcrysgro.2005.08.039.

Zavarzin, G.A., 2002. Microbial geochemical calcium cycle. Microbiology 71, 1–17. http://dx.doi.org/10.1023/A:1017945329951.